
Since January 2020 Elsevier has created a COVID-19 resource centre with free information in English and Mandarin on the novel coronavirus COVID-19. The COVID-19 resource centre is hosted on Elsevier Connect, the company's public news and information website.

Vaccine xxx (xxxx) xxx

Contents lists available at ScienceDirect

Vaccine

journal homepage: www.elsevier.com/locate/vaccine

# Protective immunity induced by an inhaled SARS-CoV-2 subunit vaccine

Elizabeth Elder [a], Chandrashekar Bangalore Revanna [b], Catharina Johansson [b], Robert P.A. Wallin [c], Johan Sjödahl [b], Ola Winqvist [b], Ali Mirazimi [a,d,*]

[a] National Veterinary Institute, Uppsala, Sweden
[b] ISR Vaccine AB, Solna, Sweden
[c] SciEd Solutions Stockholm, Sweden
[d] Clinical Microbiology, LABMED, Karolinska Institute, Sweden

ARTICLE INFO

*Article history:*
Received 7 October 2022
Received in revised form 31 May 2023
Accepted 2 June 2023
Available online xxxx

*Keywords:*
Local immunity
SARS-CoV-2
Inhaled
Respiratory tract
Dry powder
Subunit vaccine

ABSTRACT

Targeting the site of infection is a promising strategy for improving vaccine effectivity. To date, licensed COVID-19 vaccines have been administered intramuscularly despite the fact that SARS-CoV-2 is a respiratory virus. Here, we aim to induce local protective mucosal immune responses with an inhaled subunit vaccine candidate, ISR52, based on the SARS-CoV-2 Spike S1 protein. When tested in a lethal challenge hACE2 transgenic SARS-CoV-2 mouse model, intranasal and intratracheal administration of ISR52 provided superior protection against severe infection, compared to the subcutaneous injection of the vaccine. Interestingly for a protein-based vaccine, inhaled ISR52 elicited both CD4 and CD8 T-cell Spike-specific responses that were maintained for at least 6 months in wild-type mice. Induced IgG and IgA responses cross-reacting with several SARS- CoV-2 variants of concern were detected in the lung and in serum and protected animals displayed neutralizing antibodies. Based on our results, we are developing ISR52 as a dry powder formulation for inhalation, that does not require cold-chain distribution or the use of needle administration, for evaluation in a Phase I/II clinical trial.



## 1. Introduction

Mass vaccination campaigns have changed the course of the COVID-19 pandemic and reduced the morbidity and mortality associated with SARS-CoV-2 infection [1,2]. Nevertheless, waning immunity and antigenic drift will likely see the need for updated and improved vaccines that are distributed equitably across nations [3,4]. Several second-generation vaccines seek to target the site of infection, namely the respiratory tract, to induce local immunity [5–7]. These include licensed vaccines reformulated as nasal sprays [8] (Phase I clinical trial NCT04816019), and new candidates designed for intranasal administration or aerosolisation [9–20]. Preclinical results for these candidates suggest similar or better protection against SARS-CoV-2 compared with injected vaccines, with one even describing the induction of sterilizing immunity [21].

On top of the potential benefits to immunity, inhaled vaccine formulations have logistical advantages compared to injectable formulations. This is particularly true when the vaccine can be formulated as a dry powder for inhalation, completely avoiding the need for cold chain distribution [22,23]. Such a vaccine could be administered via a disposable dry powder inhaler directly into the respiratory tract, eliminating the risk of blood-borne disease transmission associated with the use of needles and syringes. Furthermore, the requirement for trained healthcare professionals is reduced. Preclinical studies using dry powder vaccines have shown promise for various pathogens and toxins including Mycobacterium tuberculosis, Human papillomavirus, and influenza A virus [24–27], and a safe and effective SARS-CoV-2 dry powder vaccine would be a boon to global vaccination efforts [4,22,23].

Here we describe the development and testing of our SARS-CoV-2 Spike S1 protein vaccine candidate ISR52. The SARS-CoV-2 Spike glycoprotein has been suggested to be an essential antigen for protective immunity against severe COVID-19 disease [28–30]. Indeed, several Spike-based subunit vaccines have shown efficacy in clinical and preclinical development [9,13–15,31]. We compare the effect of administering ISR52 via the subcutaneous, intranasal, and intratracheal route, the latter a simulation for pulmonary inhalation which to our knowledge has not previously been tested for SARS-CoV-2 vaccines.

Both respiratory routes gave 100% protection in a lethal challenge mouse model even at a low dose of ISR52, whereas only partial protection was seen with low-dose subcutaneous

* Corresponding author at: National Veterinary Institute, Uppsala, Sweden.
*E-mail address:* Ali.Mirazimi@ki.se (A. Mirazimi).

https://doi.org/10.1016/j.vaccine.2023.06.015
0264-410X/

immunisation. We find anti-Spike IgG and IgA that cross reacts with variants of concern, the induction of durable cellular immunity, and demonstrate the robustness of our platform when combining the Spike S1 protein with the adjuvant PolyICLC. Our results support the further development of ISR52 as a dry powder vaccine for inhalation.

## 2. Results and discussion

### *2.1. Respiratory administration of Spike protein vaccine ISR52 protects hACE2 transgenic mice against lethal SARS-CoV-2 challenge*

We prepared our vaccine candidate (ISR52) for administration into female AC70 hACE2 mice [32], a lethal SARS-CoV and SARS-CoV-2 infection model [32–34], where hACE2 expression is driven by the CAG promoter. Although the aim is to create an inhaled dry powder vaccine, the use of small animal models for powder inhalation was not feasible in this case. We therefore used a solution of the SARS-CoV-2 Spike protein combined with the adjuvant in our preclinical studies. The ancestral or founder SARS-CoV-2 sequence, first isolated in Wuhan, China in early 2020 [35], was used for the first vaccine formulation. We used a low and high dose of Spike protein together with poly I:C and all-trans retinoic acid (ATRA) as candidate adjuvants (Table S1). Three different routes of administration were tested: subcutaneous (s.c.) injection, intranasal (i.n.), and intratracheal (i.t.) instillation. While intranasal immunisation has been previously tested for SARS-CoV-2 vaccines [5,7,8], intratracheal administration, which simulates pulmonary inhalation, has to our knowledge not been reported, but has shown success for other pathogens [24,27,36,37]. We immunised 7 or 8 mice per group and included an additional control group of unvaccinated mice (Table S1). Two immunisations were spaced two weeks apart, and we then challenged with $2 \times 10^5$ TCID50 of founder strain SARS-CoV-2 (Fig. 1A). Prior to challenge, three mice from the high-dose intratracheal group died, one from complications from anaesthesia, and two from complications related to the i.t. administration technique. Furthermore, one mouse from the high-dose s.c. group and one from the low-dose i.t. group failed to receive complete doses of vaccines. These mice are excluded from the analysis.

After challenge, we monitored the health of all mice each day, and euthanized mice when they had lost >20% of their body weight or displayed stronger symptoms in line with our ethical permit. According to these criteria, all mice from the non–vaccinated control group were euthanized on day 4 post infection (Fig. 1B). For the low-dose s.c. group, 5/7 mice were euthanized on day 5 or 6 post infection, indicating suboptimal protection. We found 100% protection in all other groups, including at lower dose for the i.n. and i.t. groups, indicating that ISR52 raises protective immunity against SARS-CoV-2. These results are supported by analysis of change in body weight of the mice during infection (Fig. S1A). Previously published s.c. and i.n. Spike subunit vaccines have also elicited good protection in preclinical studies, but our data show that intratracheal immunisation is also an effective route of vaccine administration.

Bronchoalveolar lavage fluid (BAL), and organs were harvested from mice at the day of termination. We analysed the presence of SARS-CoV-2 RNA at the time of euthanasia in BAL and lung tissue (Fig. 1C). We detected SARS-CoV-2 RNA in BAL from mice which died during infection, including control mice and 4 mice from the low-dose s.c. group. Meanwhile, low to no detectable viral RNA was found in mice that survived (Ct > 35). We obtained similar results with lung tissue, though fewer animals overall had quantifiable SARS-CoV-2 RNA. These results indicate that the vaccinated animals, with the exception of the low dose s.c. group, either cleared the infection by day 11 post infection or that the virus never entered the lungs. We also investigated evidence of pathology in brain tissue of challenged mice, since neuronal damage is a major part of the pathology of SARS-CoV-2 in hACE2 mouse models [21,38,39]. Histopathology analysis revealed inflammation and necrosis in brain tissue for unvaccinated (8/8) and both low (5/7) and high (2/7) dose subcutaneously vaccinated groups; no similar observations were made for animals vaccinated by the respiratory routes (Fig. 1D, Table S2). These results demonstrate that both i.n. and i.t. administration of ISR52, even at low dose, protect from signs of neuronal damage in the hACE2 mouse model. Overall, we saw a clear benefit of respiratory tract vaccination versus traditional subcutaneous vaccination at low doses of ISR52.

### *2.2. SR52 immunisation induces humoral responses that cross react with variants of concern*

Since anti-Spike antibodies are likely important in protective immunity against SARS-CoV-2, we investigated the reactivity of sera from vaccinated mice collected prior to viral challenge. We analysed levels of both serum IgG and serum IgA against Spike S1 from the founder strain, and against the receptor binding domain (RBD) for the alpha variant of concern (VOC) B.1.1.7, and the beta VOC B.1.351. We found that all vaccinated groups had detectable anti-Spike IgG to at least a 1:10000 dilution for each variant, with higher dose groups demonstrating higher levels of IgG (Fig. 1E, S1B, S1C). We found larger differences between the vaccinated groups when we analysed anti-Spike IgA. Intranasal vaccination gave a stronger serum IgA response compared with intratracheal vaccination, whereas subcutaneous immunisation induced a negligible IgA titer (Fig. 1F, S1D, S1E). Since one of the aims of intranasal and intratracheal immunisation is to induce a local mucosal immune response at the relevant infection site, we also harvested BAL from animals at the time of euthanasia. We found robust anti-Spike IgA in BAL from the high dose i.n. group (Fig. 1G), with weak induction present in the s.c and i.t. groups. This pattern was reproduced when we analysed the neutralizing capacity of antibodies present in BAL (Fig. 1H). We found that subcutaneous immunisation was not associated with neutralizing activity in BAL (1 out of 13 animals in both low and high dose groups had detectable titres of neutralizing antibodies). However, we found that 44% of the intranasal and intratracheal groups had detectable levels of neutralizing antibodies up to a titre of 1 in 32 (low dose i.n. 2/8; high dose i.n. 5/7; low dose i.t. 1/7; high dose i.t. 4/5).

Taken together with survival and brain histopathology data, these antibody data suggest a more robust protection is elicited by i.n. and i.t. administration compared with s.c. immunisation. These results are consistent with previous studies of intranasal vaccination [5,8,11,13,14,21], but show for the first time evidence for the effectiveness of intratracheal immunisation against SARS-CoV-2.

### *2.3. Dose-dependent response to vaccine candidate ISR52 with variant Spike*

Following changes in predominant circulating variants, and their possible immune escape mutations, we updated our vaccine candidate to include equal amounts of alpha variant and beta variant Spike S1. We now focussed on the i.n. and i.t. administration routes and decided to lower the dose to 5 and 20 μg of total Spike S1 (Table S3), this time immunising 11 female hACE2 mice per group. We chose polyICLC as the adjuvant, which has recently been effective in an intramuscular nucleocapsid-RBD fusion subunit vaccine in hACE2 mice [40]. During this study, we harvested and analysed serum after the first and second immunisations. As expected,

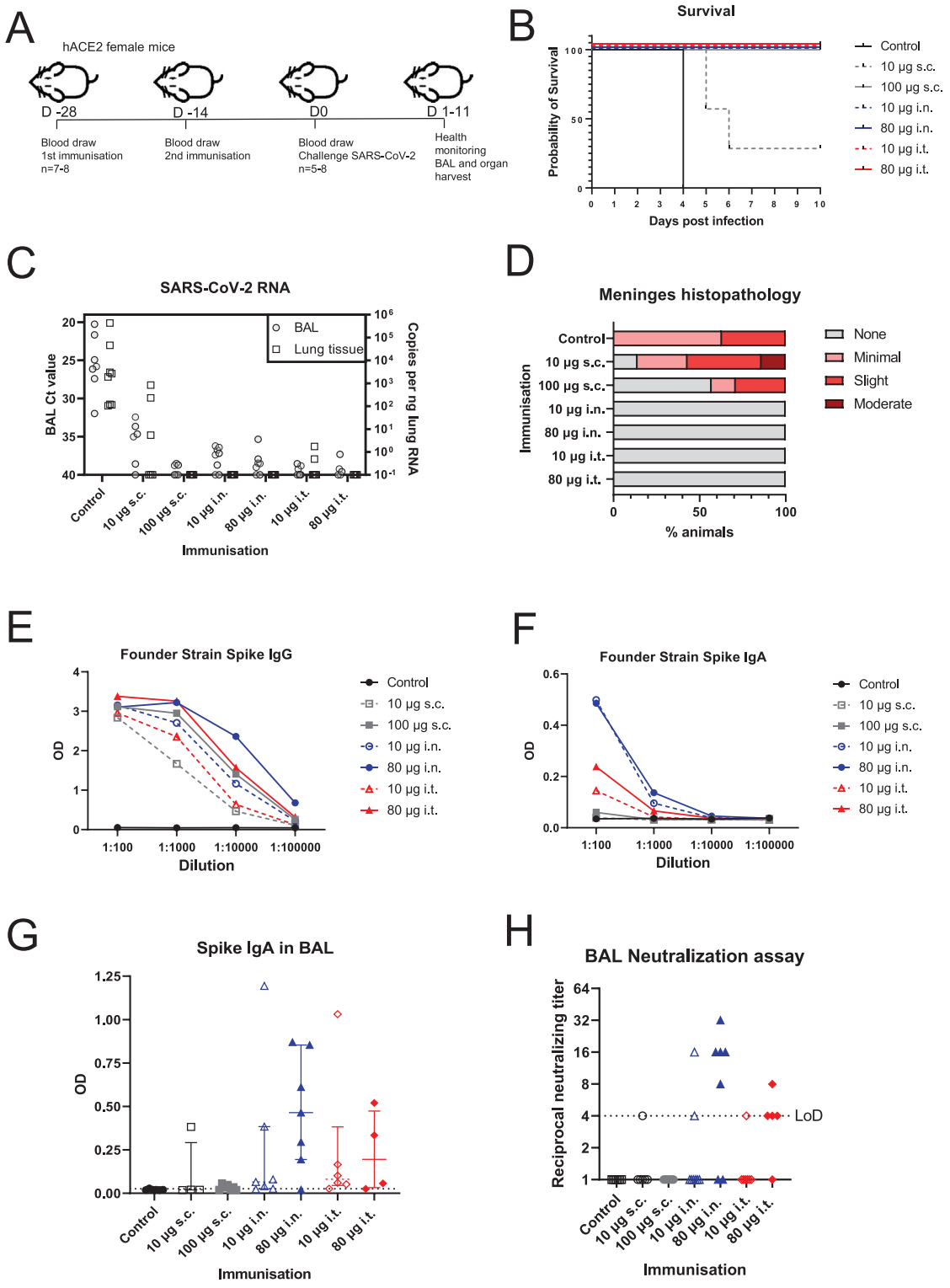


**Fig. 1.** Respiratory administration of Spike trimer vaccine protects against lethal challenge. A) Schematic showing the vaccination and challenge schedule in female K18 hACE2 mice. Mice were infected intranasally with 1.875x105 TCID SARS-CoV-2 isolate SARS-CoV-2/01/human/2020/SWE. Animals were euthanized after losing > 20% of their body mass or when other symptoms became severe. Half of the surviving animals were euthanized at 10 dpi and the other half at 11 dpi. B) Kaplan-Meier survival curve of the control and vaccinated groups. Vaccinated groups are labelled with dose of Spike trimer and the route of administration; s.c., subcutaneous; i.n., intranasal; i.t., intratracheal. The groups included the following number of animals: control n = 8, low dose s.c. n = 7, high dose s.c. n = 7, low dose i.n. n = 8, high dose i.n. n = 8, low dose i.t. n = 7, and high dose i.t. n = 5. Statistical analysis by log-rank (Mantel-Cox) test where *** indicates P < 0.001. C) SARS-CoV-2 RNA levels in BAL fluid and lung tissue at termination. 1 mL of BAL fluid for each mouse was collected at the day of euthanasia. Of this fluid, 90 µl was subjected to RNA extraction and SARS-CoV-2 E gene RT-qPCR. Ct values are plotted for each vaccine group on the left y axis. A section of lung tissue was harvested at termination for RNA and 5 ng of RNA was subsequently analysed by RT-qPCR for E gene copy number (shown on right y axis). D) Histopathology scoring of perivascular inflammatory cell infiltration in striatum-level meninges tissue from the brains of the challenged mice at termination. E) Anti-Spike S1 IgG ELISA for pre-challenge serum samples, two weeks after second immunisation. Serum was analysed for IgG against the Spike domain from SARS-CoV-2 (Founder 2020 strain first detected in Wuhan, China). F) As E, except anti-Spike S1 IgA was analysed G) Anti-Spike S1 IgA was analysed from BAL fluid harvested at termination. BAL was diluted 1:30 and the optical density (OD) is shown for individual mice. H) Neutralizing antibodies from BAL fluid at termination. BAL was then diluted beginning at 1-in-4 (LoD) and tested for neutralization of SARS- CoV-2 infection of Vero E6 cells. Results for each individual are plotted.

one immunisation gives a weak anti-Spike IgG response (Fig. 2A). The second immunisation clearly leads to a strong increase in anti-Spike IgG titre in a dose dependent manner, supporting our two-dose strategy (Fig. 2B); however, no differences between immunisation routes were observed (i.n.vs i.t.). We then investigated cross-reactivity of serum IgG and serum IgA after two immunisations, to three variant Spike RBDs, from the alpha, beta and delta variants of concern. Despite immunising with a combination of alpha and beta Spike S1 proteins, we saw similar levels of IgG and IgA against all variant RBDs within groups (Fig. 2C, S2A, S2B, S2C, S2D, S2E, S2F, S2G). Between groups, we saw evidence of dose dependency but again no significant differences between i.n. and i.t. groups of the same dose.

These serological data were complemented by analysis of neutralizing activity in pooled pre-challenge sera from each group. We found virus neutralization against the beta and the delta variant in a dose dependent manner in vaccinated mice from both i.n. and i.t. groups (Fig. 2D). Both higher dose 20 µg i.n. and i.t. groups had neutralizing titres of 1:128 and 1:64 against beta and delta, respectively, consistent with our serological data (Fig. S2B, S2C). The only

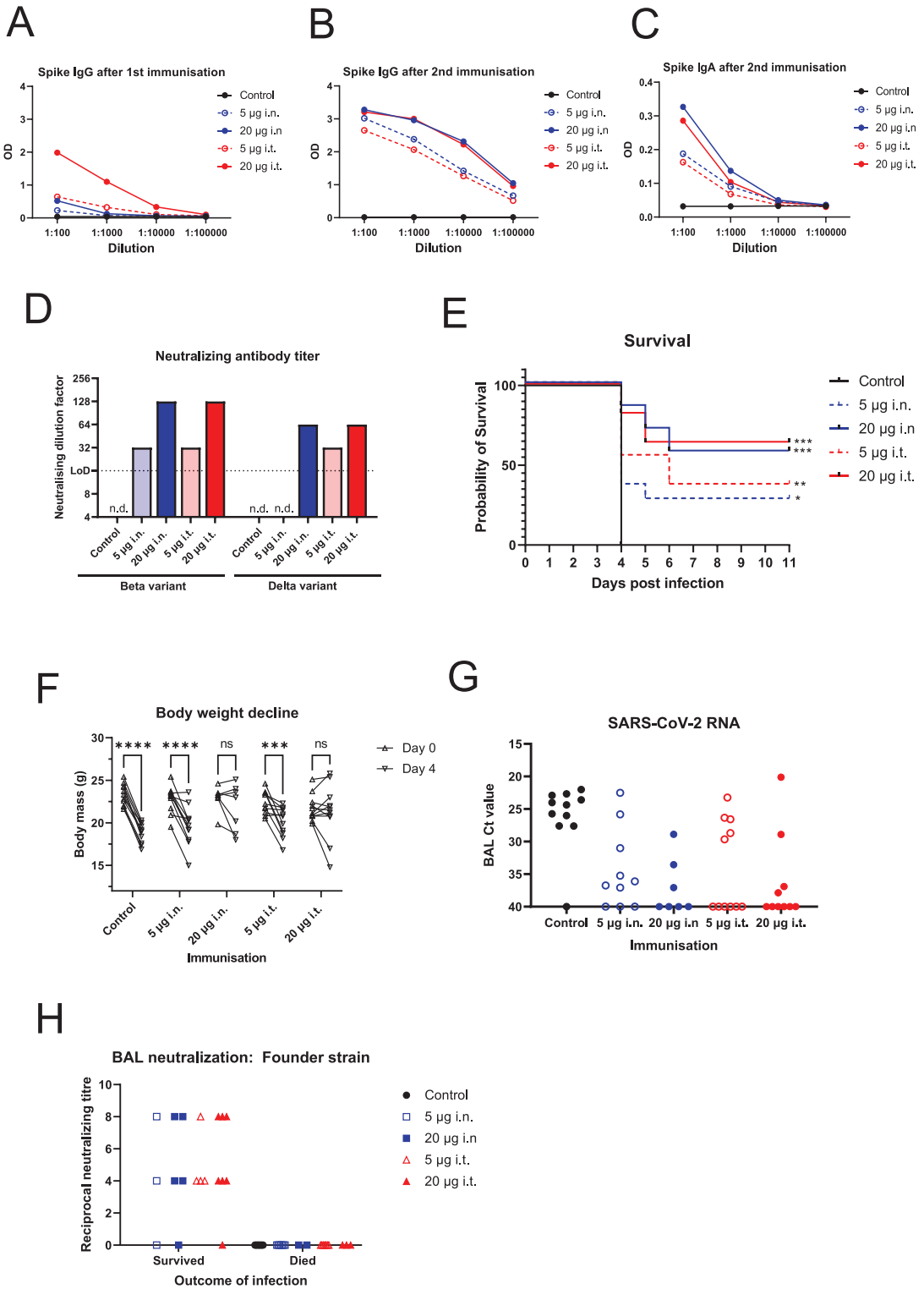

potential difference was seen with the low dose groups; low-dose i.t. showed a titre of 1 in 32 against the delta variant, but there was no detectable neutralizing antibodies in the low dose i.n. group at a detection limit of 1 in 16 (Fig. 2D).

Having observed clear pre-challenge immune responses with our updated vaccine, we decided to challenge the power of our vaccine candidate by using a higher infectious dose of SARS-CoV-2 ($1x10^6$ TCID50) compared to the first challenge study. As with the first challenge study, all control unvaccinated mice lost weight, demonstrated symptoms, and were euthanized at day 4 post infection (Fig. 2E, 2F, S2H). Unfortunately, an equipment failure led to the death of four mice in the high-dose intranasal group at 2 days post infection; the deaths of these mice were considered not related to infection and they were therefore excluded from further analysis. The low-dose groups showed a modest effect of the vaccine; 3/11 from the low-dose i.n. group and 4/11 from the low-dose i.t. group survived infection, whereas the remaining animals were euthanized on days 4, 5, or 6 (Fig. 2E). Both of these groups lost, on average, a significant proportion of their body weight by day 4 post infection (Fig. 2F). The high-dose groups showed a greater level of protection, where 4/7 of the i.n. and 7/11 of the i.t. groups survived challenge. Consistent with this, we did not observe a significant decline in weight in these mice (Fig. 2F, S2H). There was thus a clear dose-dependency of our vaccine, though we did not see differences between the route of administration by analysing health status and survival.

Finally, we analysed presence of SARS-CoV-2 RNA and neutralizing activity in BAL harvested at termination. The presence of SARS-CoV2 RNA was detectable in non-vaccinated control animals (Fig. 2G). However, in one control animal, no virus was detectable; the reason for this is unclear. In vaccinated animals, viral replicates were generally low or undetectable. However, in a few animals in each group, C(t) values similar to control animals were measured. The number of animals with low or undetectable viral titres were generally higher in high-dose groups, and in animals vaccinated via the i.t. route. The viral load was significantly correlated with survival.

As shown in Fig. 2H, we found neutralizing antibodies in the majority of protected mice, but not in susceptible mice. This strong correlation suggests that the ability of the vaccine to induce an immune response in the airways is important for its ability to protect against severe infection and death. At the same time, despite a high viral infectious dose, we did not see significant differences between intranasal and intratracheal immunisation. This could be a result of a 'common mucosal immunity' phenomenon, where immunisation at one mucosal site leads to immunity at distal sites [6,31,41,42]. One of the limitation of this present study is lack of data on vaccine efficacy against contemporarVoCs.

### *2.4. ISR52 based on Alpha Spike reveals the induction of long-term T cell and broad cross-reactive antibody responses by intranasal administration*

Our challenge studies showed the promise of vaccine candidate ISR52 when administered i.n. or i.t., inducing antibodies as well as protective immunity at low dose. We next wished to explore both humoral and cellular immune responses to our candidate, over a longer time frame, this time using Spike S1 of the alpha variant (B.1.1.7) as the antigen. We focused on i.n. and i.t. immunisation in female C57BL/6J (black 6) mice, using 5 μg and 20 μg total amount of Spike S1 in this study (Table S4). We immunised 5 or 6 mice per group at day 0 and day 14, and harvested blood, BAL, and splenocytes at day 28. Spike IgG levels in serum were dose dependent and cross reacted with the RBD of the delta VOC (B.1.617.2) and omicron VOC (B.1.1) (Fig. 3A, S3A, S3B). We found a similar pattern with BAL IgA, indicating the induction of anti-Spike IgA in a relevant tissue prior to any virus exposure (Fig. 3C, S3C, S3D), thus confirming that our immunisation strategy leads to the induction of local immune responses. These data are promising in the light of recent clinical data showing the role of cross-reactive mucosal IgA against the omicron VOC [43].

T cell responses are likely important in eliciting long-term cross-protection against severe COVID-19 disease [44], with recent reports showing protective T cell responses in the absence of detectable neutralizing antibodies in hamster and mouse models [40]. We therefore investigated if ISR52 could elicit Spike peptide- responsive T cells. We stimulated T cells from mice two weeks post second immunisation and found both IFN-γ and IL-2 producing T cells by ELISpot in all mice administered i.n. (Fig. 3C, S3E), consistent with previous analyses of intranasal COVID-19 vaccines [11,16,17,45]. Fewer mice immunised i.t. showed these responses, perhaps indicating that intranasal administration is more efficient at generating T cell responses. We found a similar pattern when analysing IFN-γ responding T cells by intracellular cytokine staining, finding both CD4+ and CD8+ populations in the higher i.n. dose group (Fig. 3D, 3E).

Next, we repeated our immunisation of C57BL/6J mice in order to follow up T cell responses over a longer period of time (Table S4). We continued to see significant CD8+ T cell responses in the higher i.n. group at 6 months post vaccination and observed a similar trend for CD4+ T cell responses (Fig. 3F, S3F). These results indicates the induction of durable CD8+ T cell response that is often a challenge for subunit vaccines [46]. These cellular responses were matched by sustained high levels of anti-RBD antibody across 6 months (Fig. 3G). In these longer term analyses, we found overall a better cellular and humoral response elicited by i.n. immunisation compared with i.t. administration.

**Fig. 2.** Dose-dependent protection from vaccination with a high infectious virus dose challenge model. A) Female hACE2 mice were immunised twice with combination alpha and beta variant Spike S1 by the indicated routes of administration. Fourteen days after the 1st immunisation, blood samples from vaccinated mice were taken and the serum diluted and analysed for IgG against the Founder strain Spike protein by ELISA. The average optical density (OD) for each vaccinated group is plotted for each dilution. B) As A, except with serum samples obtained 14 days after the 2nd immunisation. C) As B, except anti-Spike S1 IgA was analysed. D) Neutralizing activity of pre-challenge serum against variants of concern was assessed. Pre-challenge sera were pooled for each vaccinated group and tested for neutralizing activity against beta variant of concern and delta variant of concern at a starting dilution of 1-in-16 (LoD). D) Immunised mice were infected intranasally with 1.05x106 TCID SARS-CoV-2 isolate SARS-CoV-2/01/human/2020/SWE 14 days after the second immunisation. Health was monitored and animals were euthanized after losing > 20% of their body mass or when other symptoms became severe. Alternatively, surviving animals were euthanized at 11 dpi. Figure shows a Kaplan-Meier survival curve of the control and vaccinated groups. Vaccinated groups are labelled with total dose of Spike S1 and the route of administration; subcutaneous; i.n., intranasal; i.t., intratracheal. All groups included 11 animals each except high dose i.n. group that included 7 animals. Statistical analysis by log-rank (Mantel-Cox) test where * indicates $P < 0.05$, ** indicates $P < 0.01$ *** indicates $P < 0.001$ in a comparison with control animals. F) Absolute body mass of individual mice at day 0 and day 4 post infection for each group. Statistical analysis by two-way ANOVA using Sidak's multiple comparison test, ns indicates $P > 0.05$, *** indicates $P < 0.001$, **** indicates $P < 0.0001$. G) SARS-CoV-2 RNA levels in BAL fluid at termination. Equal amounts of BAL fluid for each mouse was subjected to RNA extraction and SARS-CoV-2 E gene RT-qPCR. Ct values are plotted for each vaccine group.H) Neutralizing antibodies from BAL fluid at termination. 1 mL of BAL fluid for each mouse was collected at the day of euthanasia. BAL was then diluted beginning at 1-in-4 (LoD) and tested for neutralization of SARS- CoV-2 infection (founder variant) of Vero E6 cells. Results for each individual are plotted and further divided into mice that survived to day 11 (Protected) and those that were euthanized early due to symptoms (Not protected).

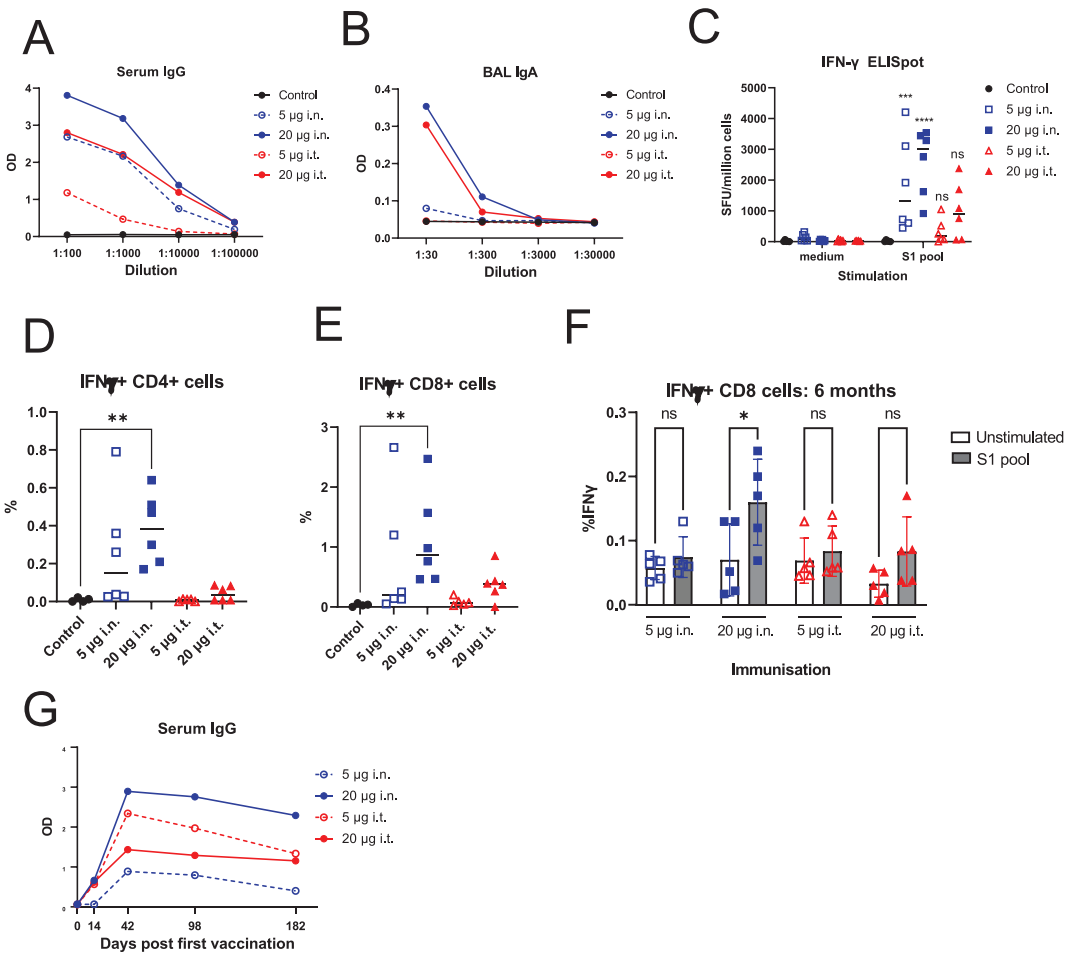


**Fig. 3.** Long-term spike-specific cellular and humoral immunity is induced by ISR52. A) Female C57BL/6J mice were immunised twice with Spike S1 alpha variant vaccine by the indicated routes of administration. Two weeks after the final immunisation, mice were euthanized and blood, BAL and spleens were harvested. Anti-alpha variant Spike RBD IgG responses in serum were assessed by ELISA, and the average optical density (OD) for each vaccinated group is plotted for each dilution of serum. B) BAL samples from mice from (A) were taken, diluted, and analysed for anti-alpha variant Spike RBD IgA by ELISA. The average optical density (OD) for each vaccinated group is plotted for each dilution. C) ELISpot analysis of T cells from spleens harvested two weeks after the second immunisation described in (A) for IFN-γ producing T cells stimulated either with medium only or by a peptide pool covering the S1 domain of the alpha variant Spike protein. Results and median for individual mice are plotted. Statistical testing by ANOVA with Sidak's multiple comparison test, where *** indicates $P < 0.001$, **** indicates $P < 0.0001$, and ns indicates $P > 0.05$ in a comparison with the corresponding medium-stimulated samples. D) T cells from vaccinated mice as per (C) were stimulated twice with S1 peptide pool or left untreated, followed by T cell marker and intracellular IFN-γ staining and flow cytometry. The proportion of IFN-γ positive CD4+ T cells is indicated. Statistical testing by ANOVA with Kruskal- Wallis multiple comparison test, where ** indicates $P < 0.01$. All other comparison were not significant. E) As (D), but showing the proportion of CD8+ T cells. F) Female C57BL/6J mice were immunised twice with Spike S1 alpha variant vaccine by the indicated routes of administration. At day 182 post initial vaccination (6 months), all animals ere euthanized, and T cells from spleens were analysed for response to S1 peptide pool as described in (D). Statistical testing by ANOVA with Sidak's multiple comparison test, where ** indicates $P < 0.01$and ns indicates $P > 0.05$. G) Serum samples from mice in (F) were analysed at the indicated times post immunisation for anti-Alpha variant Spike RBD2 IgG responses by ELISA. The average optical density (OD) for each vaccinated group is plotted for the 1:100 dilution of serum.

Overall, our modified ISR52 vaccine candidate showed good effectivity against a high dose of virus of a different strain than those to which the mice where immunised; this was true for both i.n. and i.t. administration at the higher 20 µg Spike S1 dose. Furthermore, we found long-term spike-specific humoral and cellular immune responses with the alpha Spike S1 domain administered i.n. Based on these promising virus challenge, serological, and cellular immunity data, we are moving forward with a dry powder formulation of ISR52 for inhalation in Phase I/II clinical trials.

## 3. Materials and methods

### 3.1. ISR52

The ISR52 vaccine is based on SARS-CoV-2 Spike S1 Alpha protein and the adjuvant PolyICLC. During the development of the vaccine, presented in this manuscript, different Spike variants have been evaluated. Each Spike protein was manufactured by Icosagen (Tartu, Estonia). For the first challenge study, SARS-CoV-2 trimeric Spike was used (Cat. no P-309–100); for the second challenge study, monomeric SARS-CoV-2 Spike S1 VOC 202012/K (alpha) (Cat. no P-310–100) and monomeric SARS-CoV-2 Spike S1 VOC 501.V2 (beta) (Cat. no P-319–100) were used. In the T-cell response study, monomeric SARS-CoV2 Spike S1 B.1.17 (Similar to Cat. no P-310–100, but without His-tag) was used. For the first challenge, all-trans retinoic acid (Sigma-Aldrich) was used as a supportive substance, 40 µg per mouse, with 10 µg polyIC (Invivogen) as an adjuvant. For the remaining studies, 10 µg polyICLC (Hiltonol, Oncovir) was used as an adjuvant.

### 3.2. Virus

440 SARS-CoV-2 virus strain SARS-CoV-2/01/human/2020/SWE [47] is described here as the Founder strain. SARS-CoV-2 virus strain hCoV-19/Sweden/21–51217/2021 (lineage B.1.351) [48] is described here as the beta strain. SARS-CoV-2 virus strain

SARS-CoV-2/hu/DK/SSI-H13 (lineage B.1.167.2) was provided by Dr Charlotta Polacek Strandh, Statums Serum Institut, Copenhagen, Denmark and is described here as the delta strain. All SARS-CoV-2 strains were grown and titered in a BSL-3 facility on VeroE6 cells by plaque assay [47,49] or TCID50 using the presence of cytopathic effect (CPE) as the endpoint [50].

### 3.3. Animal experiments

Female AC70 hACE2 mice [32] were purchased from Taconic, Denmark. Treatment of the mice was governed by ethical permit (reference 16765–202, approved by the regional animal experimental ethics committee in Stockholm). All animal challenge studies were conducted at Astrid Fagraeus Laboratorium in Solna, Sweden, under BSL-3 conditions by Adlego Biomedical AB. Additional animal experiments were conducted at the Adlego Biomedical AB laboratory, Department of Comparative Medicine, Karolinska University Hospital, Solna, Sweden. Isofluorane anaesthesisa was used for intransal vaccination (25 µl volume), intransal infection, euthanasia, and broncheoalveolar lavage. Ketaminol and Rompun anaesthesia was used for intratracheal vaccination, and once mice were fully anaesthetised, they were placed in a supine position. A bent 19 G steel gavage tube was used to administer 25 µl of vaccine between the vocal cords. Indicated adjuvants Poly(I:C) (HMW) (Cat. no vac-pic, Invivogen), ATRA (Cat no: R2625, Sigma Aldrich), and/or PolyICLC (Hiltonol, Oncovir Inc) were mixed with antigen just prior to immunisation. Mice were infected with the indicated infectious dose of SARS-CoV-2 intranasally in a volume of 25 µl. Health status was documented on vaccination days and daily after infection according to a modified Irwin screen.

### 3.4. Cells

VeroE6 cells were obtained from ATCC (CRL-1586) and maintained in DMEM medium supplemented with 10% fetal calf serum (FCS; Gibco), 1% Non-essential amino acids (Gibco), and 10 mM HEPES (Gibco) at 37 °C in a 5% $CO_2$ humidified atmosphere.

### 3.5. Microneutralization assay

VeroE6 cells were seeded on 96 well plates at a seeding density of $2x10^4$ cells per well one day prior to infection. BAL or serum was heat inactivated for 30 min at 56 °C before dilution in DMEM medium supplemented with 2% FCS, 100 units/mL of penicillin and 100 µg/mL streptomycin. The diluted BAL/serum was then distributed in triplicate into 96 well round bottom plates and mixed with 500 plaque forming units of SARS-CoV-2 per well, and incubated at 37 °C/5% $CO_2$ for 1 h. Medium from the VeroE6 cells was aspirated and replaced with virus:BAL/serum mix. Virus only, BAL/serum only, and convalescent patient serum controls were included. After 3 days' incubation at 37 °C/5% $CO_2$, the presence of CPE was checked. Neutralizing activity was assigned to wells which showed a complete absence of CPE. The neutralizing titer was then calculated as the dilution factor where >50% of wells showed neutralizing activity.

### 3.6. ELISA

Clear flat bottom immuno nonsterile 96 well polystyrene plates (Thermo Scientific) were coated with either founder strain Spike S1, alpha variant RBD2, beta variant RBD2, delta variant RBD2, or omicron variant RBD2 purchased from Icosagen (Tartu, Estonia) at 5 µg/ml in PBS 1X buffer, pH 7.2, using 50 µl/well. The plates were covered with sealing tape, incubated overnight at 4 °C and then washed with PBS + 0.05% Tween 20. Blocking was performed by applying 150 µl/well of diluent solution for 1 h at RT and plates were then washed. 100 µl of serum diluted in diluent solution were applied per well, incubated for 2 h at RT, followed by washing. Detection antibody, 100 µl/well, diluted 1:1000 in diluent was added and incubated for 1 h at RT. For IgG, conjugated anti-mouse IgG alkaline phosphatase (ALP) (Cat. no 3310–4, Mabtech) was used, and for IgA first biotinylated anti-mouse IgA (100 µl/well, diluted 1:1000 in diluent) (Cat. no 3865–6, Mabtech) and then streptavidin ALP (100 µl/well, diluted 1:1000 in diluent) (Cat. no 3310–8, Mabtech) was added and incubated for 1 h at RT. After washes, 100 µl pNPP substrate per well was added, the enzymatic reaction was developed for 30 min and analyte absorbance (410 nm) and background absorbance (620 nm) measured by a BMG LABTECH FLUOstar omega ELISA plate reader. Results were considered positive when the optical density (OD) obtained with the ELISA was three times higher than the negative control. All antibodies, the diluent solution and the pNPP substrate were from Mabtech.

### 3.7. IL-2 and IFN-γ ELISpot

IL-2 and IFN-γ ELISpot reagents were purchased from Mabtech and the assays were performed according to manufacturer instructions. Mabtech's mouse IL-2 ELISpot PLUS kit (ALP) and mouse IFN-γ ELISpot PLUS kit (ALP) were used for detection of IL2 and IFN-γ, respectively. The precoated plates are washed 4 times with sterile PBS pH 7.2 (Gibco Life Technologies Limited) and conditioned by blocking with 10/90% FBS/RPMI 1640 Glutamax (Gibco Life Technologies Limited) for at least 30 min at room temperature. SARS-CoV-2 S1 scanning pool antigen stimuli stock solution (Mabtech), 200 µg/ml, was prepared from the lyophilized peptide pool by addition of 40 µl of DMSO and 85 µl PBS followed by further dilution in cell culture medium giving a peptide concentration of 2 µg/ml. Conditioning medium was removed from the plates and 100 µl of peptide pool, followed by 100 µl of cell suspension, such that 250,000 mouse splenocytes were stimulated per well. The plates were incubated at 37 ºC, 5% $CO_2$ for 15–18 h for IL2 plates and 32–35 h for IFN-γ plates. The next day cells were removed and the plates washed five times followed by incubation with 100 µl/well of detection antibody (5H4-biotin) diluted to 1 µg/ml in PBS containing 0.5 % FBS, for IL-2 detection and detection antibody R4-6A2-biotin for IFN-γ detection, for 2 h at room temperature. The plates were then washed five times with PBS followed by incubation with 100 µl/well of Streptavidin-ALP diluted 1:1000 in PBS containing 0.5 % FBS. After incubation at room temperature for 1 h, the plates were washed as before and 100 µl/well of the substrate (BCIP/NBT-plus) was added and the plates incubated for 15 min at room temperature in the dark. After extensive washing in tap water, the plates were dried overnight before detection of spot forming units using either an IRIS or ASTOR ELISpot instrument.

### 3.8. In vitro proliferation and intracellular cytokine staining (ICS) analysis by flow cytometry

Splenocytes from vaccinated and control mice were prepared and stained with CellTrace Violet dye according to the manufacturers instructions (ThermoFisher Scientific, MA, USA). One million splenocytes were then stimulated or left untreated for 4 days in wells of a flat bottom 96 well plate in duplicate. After 4 days, the cells were restimulated with antigen for a further 24 h. At 6–8 h prior to harvesting, protein transport inhibitor cocktail was added to the cells (ThermoFisher Scientific). The cells were harvested and the duplicate wells pooled into V bottom 96 well plates to reduce cell loss during the intracellular staining. The cell samples were then stained with T-cell surface markers (CD3 FITC, CD8 PerCp-Cy5.5, CD4 APC, all ThermoFisher Scientific) followed by intracellu-

lar staining of IFN-gamma (IFN-γ PE clone XMG1.2. ThermoFisher Scientific) using the intracellular fix/perm kit (ThermoFisher Scientific) according to the manufacturer's instructions. The samples was analyzed with a MACSQuant16 instrument (Miltenyi Biotech).

### 3.9. SARS-CoV-2 RT-qPCR

Equal volumes of BAL from each mouse was mixed with Trizol (Thermo Fisher). RNA was extracted using Direct Zol RNA mini kit (Zymo Research), and analyzed for the content of SARS-CoV-2 RNA by RT-qPCR using the following primers/probes as previously described [47]. SARS-CoV-2 E gene: forward: ACAGGTACGTTAATAGTTAATAGCGT; reverse: ATATTGCAGCAGTACGCACACA; probe: FAM- ACACTAGCCATCCTTACTGCGCTTCG-MGB.

Lung tissue was lysed in Trizol and RNA was extracted using Direct Zol RNA mini kit (Zymo research). The copy number of SARS-CoV-2 RNA was determined by analysing 5 ng of RNA from each lung tissue sample, using E gene RNA transcripts of a defined copy number (EDX SARS-CoV-2 Standard, Biorad) to generate a standard curve. Primers and probes as above.

### 3.10. Histopathology

Histopathology analysis was performed by BioVet AB. Brain tissue was harvested and fixed in 4% formaldehyde and sectioned (between 4 and 6 μm). Sections were stained with haematoxylin-eosin and scored for histopathological changes according to distribution, severity (miminal, slight, moderate, marked, and severe), and morphologic character.

## Data availability

Data will be made available on request.

## Declaration of Competing Interest

The authors declare the following financial interests/personal relationships which may be considered as potential competing interests: EE and AM declare no competing interests. C.B.R., C.J., J. S., and O.W. are employed by Immune System Regulation AB (ISR). R.P.A.W. is a consultant working for ISR. O.W. and J.S. are shareholders in ISR, and O.W. is the founder of ISR. ISR have registered a patent based on the vaccine candidate described in this manuscript.

## Appendix A. Supplementary data

Supplementary data to this article can be found online at https://doi.org/10.1016/j.vaccine.2023.06.015.

## References

[1] Zheng C et al. Real-world effectiveness of COVID-19 vaccines: a literature review and meta-analysis. Int J Infect Dis 2021.
[2] Kandimalla R et al. Counting on COVID-19 vaccine: insights into the current strategies. Prograd Fut Challen Biomed 2021;9(11).
[3] Milne G et al. Does infection with or vaccination against SARS-CoV-2 lead to lasting immunity? Lancet Respir Med 2021;9(12):1450–66.
[4] Van De Pas R et al. COVID-19 vaccine equity: a health systems and policy perspective. Expert Rev Vaccines 2021:1–12.
[5] Chavda VP et al. Intranasal vaccines for SARS-CoV-2: From challenges to potential in COVID-19 management. Drug Discov Today 2021;26 (11):2619–36.
[6] Lavelle EC, Ward RW. Mucosal vaccines - fortifying the frontiers. Nat Rev Immunol 2021.
[7] Alu A et al. Intranasal COVID-19 vaccines: From bench to bed. EBioMedicine 2022;76:103841.
[8] Doremalen NV et al. Intranasal ChAdOx1 nCoV-19/AZD1222 vaccination reduces viral shedding after SARS-CoV-2 D614G challenge in preclinical models. Sci Transl Med 2021;13(607):eabh0755.
[9] Guebre-Xabier M et al. NVX-CoV2373 vaccine protects cynomolgus macaque upper and lower airways against SARS-CoV-2 challenge. Vaccine 2020;38 (50):7892–6.
[10] Kumar US et al. Gold-nanostar-chitosan-mediated delivery of SARS- CoV-2 DNA vaccine for respiratory mucosal immunization: development and proof-of-principle. ACS Nano 2021.
[11] Hassan AO et al. A single-dose intranasal ChAd vaccine protects upper and lower respiratory tracts against SARS-CoV-2. Cell 2020;183(1):169–84. e13.
[12] Wu S et al. Safety, tolerability, and immunogenicity of an aerosolised adenovirus type-5 vector-based COVID-19 vaccine (Ad5-nCoV) in adults: preliminary report of an open-label and randomised phase 1 clinical trial. Lancet Infect Dis 2021;21(12):1654–64.
[13] Sui Y et al. Protection against SARS-CoV-2 infection by a mucosal vaccine in rhesus macaques. JCI Insight 2021;6(10).
[14] Du Y et al. Intranasal administration of a recombinant RBD vaccine induced protective immunity against SARS-CoV-2 in mouse. Vaccine 2021;39 (16):2280–7.
[15] van der Ley PA et al. An intranasal OMV-based vaccine induces high mucosal and systemic protecting immunity against a SARS-CoV-2 infection. Front Immunol 2021;12:781280.
[16] O'Donnell KL et al. Optimization of single-dose VSV-based COVID-19 vaccination in hamsters. Front Immunol 2021;12:788235.
[17] Chung NH et al. Induction of Th1 and Th2 in the protection against SARS-CoV-2 through mucosal delivery of an adenovirus vaccine expressing an engineered spike protein. Vaccine 2022;40(4):574–86.
[18] Liu X et al. A single intranasal dose of a live-attenuated parainfluenza virus-vectored SARS-CoV-2 vaccine is protective in hamsters. Proc Natl Acad Sci USA 2021;118(50).
[19] Stark FC et al. Intranasal immunization with a proteosome-adjuvanted SARS-CoV-2 spike protein-based vaccine is immunogenic and efficacious in mice and hamsters. Sci Rep 2022;12(1).
[20] Afkhami S et al. Respiratory mucosal delivery of next-generation COVID-19 vaccine provides robust protection against both ancestral and variant strains of SARS-CoV-2. Cell 2022;185(5):896–915. e19.
[21] Ku MW et al. Brain cross-protection against SARS-CoV-2 variants by a lentiviral vaccine in new transgenic mice. EMBO Mol Med 2021:e14459.
[22] AboulFotouh K, Cui Z, Williams 3rd RO. Next-generation COVID-19 vaccines should take efficiency of distribution into consideration. AAPS PharmSciTech 2021;22(3):126.
[23] Heida R, Hinrichs WL, Frijlink HW. Inhaled vaccine delivery in the combat against respiratory viruses: a 2021 overview of recent developments and implications for COVID-19. Expert Rev Vaccines 2021:1–18.
[24] Kesarwani A et al. The safety and efficacy of BCG encapsulated alginate particle (BEAP) against M.tb H37Rv infection in Macaca mulatta: A pilot study. Sci Rep 2021;11(1):3049.
[25] Bahamondez-Canas TF, Cui Z. Intranasal immunization with dry powder vaccines. Eur J Pharm Biopharm 2018;122:167–75.
[26] Luczo JM et al. Intranasal powder live attenuated influenza vaccine is thermostable, immunogenic, and protective against homologous challenge in ferrets. NPJ Vaccines 2021;6(1):59.
[27] Rossi I et al. A respirable HPV-L2 dry-powder vaccine with GLA as amphiphilic lubricant and immune-adjuvant. J Control Release 2021;340: 209–20.
[28] Fergie J, Srivastava A. Immunity to SARS-CoV-2: lessons learned. Front Immunol 2021;12:654165-654165.
[29] Shrock E et al. Viral epitope profiling of COVID-19 patients reveals cross-reactivity and correlates of severity. Science (New York, N.Y.) 2020;370(6520): eabd4250.
[30] Robbiani DF et al. Convergent antibody responses to SARS-CoV-2 in convalescent individuals. Nature 2020;584(7821):437–42.
[31] Jearanaiwitayakul T et al. Peritoneal administration of a subunit vaccine encapsulated in a nanodelivery system not only augments systemic responses against SARS-CoV-2 but also stimulates responses in the respiratory tract. Viruses 2021;13(11).
[32] Tseng CT et al. Severe acute respiratory syndrome coronavirus infection of mice transgenic for the human Angiotensin-converting enzyme 2 virus receptor. J Virol 2007;81(3):1162–73.
[33] Xu G et al. SARS-CoV-2 promotes RIPK1 activation to facilitate viral propagation. Cell Res 2021:1–14.
[34] Yoshikawa N et al. Differential virological and immunological outcome of severe acute respiratory syndrome coronavirus infection in susceptible and resistant transgenic mice expressing human angiotensin-converting enzyme 2. J Virol 2009;83(11):5451–65.
[35] Zhou P et al. A pneumonia outbreak associated with a new coronavirus of probable bat origin. Nature 2020;579(7798):270–3.
[36] Feng J et al. Construction of a live-attenuated vaccine strain of yersinia pestis EV76-B-SHUΔpla and evaluation of its protection efficacy in a mouse model by aerosolized intratracheal inoculation. Front Cell Infect Microbiol 2020;10. 473–473.
[37] Griffiths GD et al. Liposomally-encapsulated ricin toxoid vaccine delivered intratracheally elicits a good immune response and protects against a lethal pulmonary dose of ricin toxin. Vaccine 1997;15(17–18):1933–9.

[38] Golden JW et al. Human angiotensin-converting enzyme 2 transgenic mice infected with SARS-CoV-2 develop severe and fatal respiratory disease. JCI Insight 2020;5(19).
[39] Rathnasinghe R et al. Comparison of transgenic and adenovirus hACE2 mouse models for SARS-CoV-2 infection. Emerg Microbes Infect 2020;9(1):2433–45.
[40] Castro JT et al. Promotion of neutralizing antibody-independent immunity to wild-type and SARS-CoV-2 variants of concern using an RBD- Nucleocapsid fusion protein. Nat Commun 2022;13(1):4831.
[41] van Splunter M et al. Oral cholera vaccination promotes homing of IgA(+) memory B cells to the large intestine and the respiratory tract. Mucosal Immunol 2018;11(4):1254–64.
[42] Weisz-Carrington P et al. Organ and isotype distribution of plasma cells producing specific antibody after oral immunization: evidence for a generalized secretory immune system. J Immunol 1979;123(4):1705–8.
[43] Havervall S et al. Anti-spike mucosal IgA protection against SARS- CoV-2 omicron infection. N Engl J Med 2022.
[44] Moss P. The T cell immune response against SARS-CoV-2. Nat Immunol 2022;23(2):186–93.
[45] Pillet S et al. Safety, immunogenicity, and protection provided by unadjuvanted and adjuvanted formulations of a recombinant plant-derived virus-like particle vaccine candidate for COVID-19 in nonhuman primates. Cell Mol Immunol 2022;19(2):222–33.
[46] Ho NI et al. Adjuvants enhancing cross-presentation by dendritic cells: The key to more effective vaccines? Front Immunol 2018;9:2874.
[47] Monteil V et al. Inhibition of SARS-CoV-2 infections in engineered human tissues using clinical-grade soluble human ACE2. Cell 2020;181(4):905–913 e7.
[48] Normark J et al. Heterologous ChAdOx1 nCoV-19 and mRNA-1273 Vaccination. N Engl J Med 2021;385(11):1049–51.
[49] Becker MM et al. Synthetic recombinant bat SARS-like coronavirus is infectious in cultured cells and in mice. Proc Natl Acad Sci 2008;105 (50):19944–9.
[50] Wulff NH, Tzatzaris M, Young PJ. Monte Carlo simulation of the Spearman-Kaerber TCID50. J Clin Bioinf 2012;2(1):5.